JOURNAL OF GUIDANCE, CONTROL, AND DYNAMICS
Vol. 19, No. 3, May–June 1996

Stability Analysis on Earth Observing System AM-1 Spacecraft Earth Acquisition

Xipu Li* and Arthur J. Throckmorton†
Lockheed Martin Astro Space, Princeton, New Jersey 08543
and
Jeffrey B. Boka‡
Lockheed Martin Astro Space, King of Prussia, Pennsylvania 19046-2902

The design and analysis of the Earth Observing System AM-1 spacecraft Earth acquisition mode are presented. In addition to addressing the practical design of the spacecraft attitude control system, some mathematical proofs of the system stability based on the spacecraft nonlinear dynamics and kinematics are demonstrated. The main approach of the analysis is to identify all of the equilibrium points of the closed-loop system and then to investigate the stability of each of the equilibrium points. Since it is not restricted to near the nominal operating point, this work extends the previous linear analysis results to certain cases where large attitude errors are possible. All three control configurations in the Earth acquisition mode are investigated. The system convergence from any yaw attitude to the nominal Earth pointing attitude is proven. The results developed in the paper provide a deeper understanding of the system dynamics and are especially useful in analyzing off-nominal launch-vehicle/spacecraft separations and in determining submode transition thresholds. The design and analysis are supported by high-fidelity spacecraft simulation.

Nomenclature

$A_{zxy}(\boldsymbol{e})$ or $A_{zxy}(\theta_x, \theta_y, \theta_z)$ = transformation matrix corresponding to the Euler angle $\boldsymbol{e}$ with the z–x–y rotation sequence

$\boldsymbol{e}$ = spacecraft attitude error vector $\begin{bmatrix}\theta_x\\ \theta_y\\ \theta_z\end{bmatrix}$ defined as the Euler angles from its nominal attitude with the z–x–y rotation sequence

I = spacecraft inertia matrix $\begin{bmatrix} I_{xx} & -I_{xy} & -I_{xz}\\ -I_{xy} & I_{yy} & -I_{yz}\\ -I_{xz} & -I_{yz} & I_{zz}\end{bmatrix}$

$S = \text{span}\{\boldsymbol{v}_1, \ldots, \boldsymbol{v}_n\}$ = linear vector subspace spanned by vectors $\{\boldsymbol{v}_1, \ldots, \boldsymbol{v}_n\}$

$\boldsymbol{w}$ = spacecraft angular velocity vector $\begin{bmatrix}\omega_x\\ \omega_y\\ \omega_z\end{bmatrix}$ defined in the spacecraft body frame

$\|\boldsymbol{v}\|$ = 2-norm of a vector $\boldsymbol{v} = \begin{bmatrix}v_x\\ v_y\\ v_z\end{bmatrix}$ defined as $\|\boldsymbol{v}\| := \sqrt{(v_x^2 + v_y^2 + v_z^2)}$

$[\boldsymbol{v}]_s$ = skew symmetric matrix of a vector $\boldsymbol{v} = \begin{bmatrix}v_x\\ v_y\\ v_z\end{bmatrix}$ defined as $\begin{bmatrix} 0 & -v_z & v_y\\ v_z & 0 & -v_x\\ -v_y & v_x & 0\end{bmatrix}$

0_3 = 3×3 zero matrix

1_3 = 3×3 identity matrix

Received Sept. 29, 1995; revision received Jan. 2, 1996; accepted for publication Jan. 3, 1996.

*Staff Systems Engineer, Guidance, Navigation, and Control, M/S WC-2, P.O. Box 800. Member AIAA.
†Section Manager, Guidance, Navigation, and Control, M/S WC-2, P.O. Box 800. Senior Member AIAA.
‡Staff Systems Engineer, Guidance, Navigation, and Control, M/S U2101.

I. Introduction

THE Earth Observing System (EOS) spacecraft series is the cornerstone of NASA's Mission to Planet Earth. The first spacecraft, EOS AM-1 (see Fig. 1), is currently being developed by Lockheed Martin Astro Space and is scheduled for launch on an Atlas Launch Vehicle in June 1998.

The mission of the EOS AM-1 spacecraft requires that the attitude control system have a highly accurate Earth-pointing controllability (less than several tens of arcseconds) when the spacecraft (SC) is orbiting the Earth. The attitude control operation through the mission is mainly composed of two major modes: initial Earth acquisition mode and normal control mode. The Earth acquisition mode is an initial coarse attitude control process, the primary goal of which is to align the spacecraft body (SCB) frame with its target frame, the local vertical local horizontal (LVLH) frame, after launch-vehicle/spacecraft (LV/SC) separation. During this mode, the SC will be controlled based on its attitude errors and rate errors. The attitude is measured by two earth sensor assemblies (ESAs) and the rate is measured by an inertial reference unit (IRU) consisting of two sets of three-axis gyros. Once the spacecraft body frame is roughly aligned with the LVLH frame (the attitude error is less than 4 degs in each axis), the spacecraft controls computer (SCC) will be switched to the normal control mode where an attitude estimator

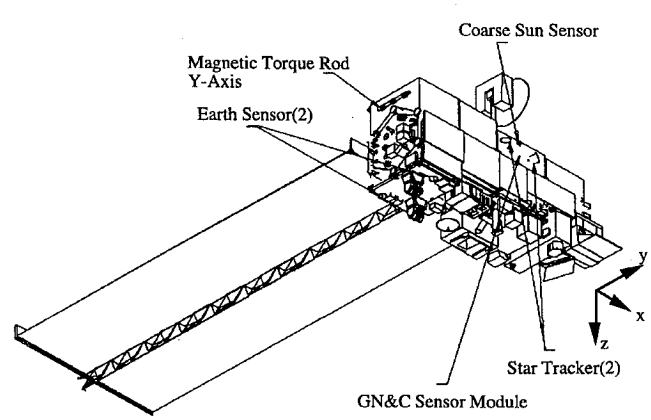

Fig. 1 EOS AM-1 spacecraft: x axis = roll, y axis = pitch, and z axis = yaw.

will be used to provide more accurate SC attitude information using star measurements. This paper will describe the Earth acquisition control mode.

The Earth acquisition control mode can be further divided into three submodes: rate nulling submode, local vertical acquisition submode, and yaw acquisition submode. Following LV/SC separation, the SCC will start the rate nulling submode and the IRU will start to measure the SC body rates. If the separation causes the body rates to be greater than a threshold of 0.04 deg/s in each axis, six (1)-lbf attitude control thrusters will be fired to reduce the rates below the threshold prior to transition to local vertical acquisition submode. Otherwise, the system will be switched to the local vertical acquisition submode autonomously. The goal of the local vertical acquisition submode is to align the SC yaw axis (z axis) with the nadir vector. While the IRU continues to provide all three axis rates, two conical ESAs are used to measure the SC roll and pitch errors. Based on these five error signals, a control torque is generated from the reaction wheel assembly (RWA) such that the SC z axis is slewed toward the nadir vector through momentum exchange. In this submode, the SC yaw angle is not being controlled; therefore, large yaw errors may be present. Once the SC yaw axis is aligned with the nadir vector, the yaw acquisition submode will be entered and the yaw attitude error signal will be derived from the roll and pitch rates (yaw gyrocompassing). Based on the six attitude and rate error signals, the control system will generate control torques from the RWA to maintain the SC in its nominal Earth pointing attitude. The initial Earth acquisition is completed when attitude errors are less than 4 deg and rate errors are less than 0.02 deg/s in each axis.

Classical control techniques were the major tool employed in the EOS AM-1 spacecraft Earth acquisition design. The design process proceeded as follows. First, the SC dynamic and kinematic equations were linearized at the nominal operating point. Then a feedback proportional plus derivative (PD) control gain matrix was selected such that certain stability margins were achieved for each axis.[1,2] However, the results from this linear analysis only guarantee that the closed-loop system is stable when it is near the nominal operating point; no further conclusion can be drawn on how large the stability region is and where the SC attitude would converge if large attitude errors occurred. In particular, it is important to answer questions such as whether the SC would converge to its nominal attitude from the 90- or 180-deg yaw position, with or without the yaw gyrocompassing applied.

This paper provides a further analysis to address these issues. The analysis is based on the SC nonlinear dynamic and kinematic equations. Under the assumption that the spacecraft is facing down to the Earth immediately after LV/SC separation, all equilibrium points of the closed-loop system are identified. Then the stability of each of these equilibrium points is investigated. This approach is applied to all three control configurations in the Earth acquisition mode, and the system convergence from an arbitrary yaw attitude to the nominal Earth pointing attitude is proven. In addition to providing a deeper understanding of the system dynamics, the results developed in the paper are especially useful in analyzing off-nominal LV/SC separations and in determining submode transition thresholds.

The remainder of the paper is organized as follows. Sections II and III provide the modeling and design of the EOS AM-1 spacecraft attitude control system, respectively. All equilibrium points of the closed-loop system are identified in Sec. IV. Section V investigates the stability of these equilibrium points and the system convergence to the nominal operating point. Section VI is a summary.

II. Mathematical Model

Referring to Fig. 1, the SCB frame is defined as x axis is equal to roll axis, y axis is equal to pitch axis, and z axis is equal to yaw axis. Through the mission life, the spacecraft nominal attitude is aligned with the SC centered LVLH frame, which is defined as y axis is aligned with the negative orbit normal vector, z axis is pointing to the center of the Earth (nadir vector), and x axis is such that the x, y, z axes are right-hand orthogonal. The LVLH frame rotates about its y axis at the orbit rate as the spacecraft is orbiting the Earth. In the EOS AM-1 mission, the nominal spacecraft rate vector is

Table 1 EOS AM-1 mass properties

Description	Inertia, slug-ft^2					
	I_{xx}	I_{yy}	I_{zz}	I_{xy}	I_{xz}	I_{yz}
All stowed	3508.02	13907.0	13088.1	49.28	605.07	−31.27
Solar array blanket deployed high-gain antenna stowed	8111.0	14010.0	17576.0	−205.98	517.54	573.89
All deployed beginning of life	8946.47	13855.7	16586.7	−208.08	409.66	568.93

$$\boldsymbol{w}_0 = \begin{bmatrix} 0 \\ \Omega \\ 0 \end{bmatrix} \tag{1}$$

where $\Omega = -0.001$ rad/s. The fundamental SC dynamic equation is Euler's moment equation[3]

$$I\dot{\boldsymbol{w}} + [\boldsymbol{w}]_\times I\boldsymbol{w} = \boldsymbol{u} + \boldsymbol{d} \tag{2a}$$

or

$$\dot{\boldsymbol{w}} = -I^{-1}[\boldsymbol{w}]_\times I\boldsymbol{w} + I^{-1}\boldsymbol{u} + I^{-1}\boldsymbol{d} := \boldsymbol{f}_1(\boldsymbol{w}, \boldsymbol{u}, \boldsymbol{d}) \tag{2b}$$

where I is the spacecraft inertia matrix (given in Table 1), $\boldsymbol{w}$ the spacecraft rate vector, $\boldsymbol{u}$ the applied control torque vector, and $\boldsymbol{d}$ the external disturbance torque vector, all of which are defined in the SCB frame.

In the following derivations, the z–x–y rotation sequence is selected. The advantage of this selection is that the ESAs output signals are consistent with the SC roll and pitch attitude error definitions for any yaw errors. Using this rotation sequence, the transformation matrix from the LVLH frame to the SCB frame is[3]

$$A_{zxy}(\theta_x, \theta_y, \theta_z) = \begin{bmatrix} \cos\theta_y \cos\theta_z - \sin\theta_x \sin\theta_y \sin\theta_z & \cos\theta_y \sin\theta_z + \sin\theta_x \sin\theta_y \cos\theta_z & -\cos\theta_x \sin\theta_y \\ -\cos\theta_x \sin\theta_z & \cos\theta_x \cos\theta_z & \sin\theta_x \\ \sin\theta_y \cos\theta_z + \sin\theta_x \cos\theta_y \sin\theta_z & \sin\theta_y \sin\theta_z - \sin\theta_x \cos\theta_y \cos\theta_z & \cos\theta_x \cos\theta_y \end{bmatrix} \tag{3}$$

and the kinematic equation is[3]

$$\dot{\boldsymbol{e}} = \begin{bmatrix} \dot{\theta}_x \\ \dot{\theta}_y \\ \dot{\theta}_z \end{bmatrix} = \begin{bmatrix} \cos\theta_y & 0 & \sin\theta_y \\ \dfrac{\sin\theta_x \sin\theta_y}{\cos\theta_x} & 1 & \dfrac{-\sin\theta_x \cos\theta_y}{\cos\theta_x} \\ \dfrac{-\sin\theta_y}{\cos\theta_x} & 0 & \dfrac{\cos\theta_y}{\cos\theta_x} \end{bmatrix} \boldsymbol{v} \tag{4}$$

where $\boldsymbol{v}$ is an SCB frame vector representing the SC angular velocity relative to the LVLH frame. Since the LVLH frame rotates about the nominal orbit rate vector $\boldsymbol{w}_0$, and $\boldsymbol{w}_0$ is defined in the LVLH frame, we have

$$\boldsymbol{v} = \boldsymbol{w} - A_{zxy}(\boldsymbol{e})\boldsymbol{w}_0 \tag{5}$$

III. Earth Acquisition Control System Design

The EOS AM-1 Earth acquisition attitude control system is designed on the linearized model at its nominal operating point.

Taking the derivative of f_1 in Eq. (2b) with respect to w and u, we have

$$\dot{w} = f_1(w_0, u_0) + \frac{\partial f_1}{\partial w}(w_0, u_0)\Delta w + \frac{\partial f_2}{\partial u}(w_0, u_0)\Delta u \quad (6a)$$

$$\Delta w = w - w_0 \quad (6b)$$

$$\Delta u = u - u_0 \quad (6c)$$

$$\frac{\partial f_1}{\partial w}(w, u) = I^{-1}([Iw]_s - [w]_s I) \quad (6d)$$

$$\frac{\partial f_1}{\partial u}(w, u) = I^{-1} \quad (6e)$$

where u_0 is the nominal control torque. Based on the fact that a linear system's stability is independent of its external input, the disturbance torque d has been omitted. Moreover, since

$$\dot{w}_0 = f_1(w_0, u_0) = -I^{-1}[w_0]_s I w_0 + I^{-1}u_0 = 0 \quad (7)$$

the nominal control torque can be solved as $u_0 = [w_0]_s I w_0$, which is the SC gyroscopic torque compensation. If we assume that I is a principal axis inertia matrix (i.e., diagonal), then it is easy to see that

$$u_0 = [w_0]_s I w_0 = 0 \quad (8)$$

From Eqs. (6), the linearized dynamic equation can be expressed as

$$\Delta\dot{w} = I^{-1}([Iw_0]_s - [w_0]_s I)\Delta w + I^{-1}\Delta u \quad (9)$$

Moreover, for small Euler angles from the LVLH frame to the SCB frame, Eqs. (4) and (5) can be linearized as

$$\dot{e} \cong w - A_{zxy}(e)w_0 \cong w - (1_3 - [e]_s)w_0 = \Delta w - [w_0]_s e \quad (10)$$

Using state–space representation, the linear open-loop system can be expressed as

$$\begin{bmatrix} \Delta\dot{w} \\ \dot{e} \end{bmatrix} = A_0 \begin{bmatrix} \Delta w \\ e \end{bmatrix} + B_0 \Delta u \quad (11a)$$

where

$$A_0 = \begin{bmatrix} I^{-1}([Iw_0]_s - [w_0]_s I) & 0_3 \\ 1_3 & -[w_0]_s \end{bmatrix} \quad (11b)$$

$$B_0 = \begin{bmatrix} I^{-1} \\ 0_3 \end{bmatrix} \quad (11c)$$

Note that after the solar array is deployed, the SC spin axis becomes the intermediate axis; therefore, the open-loop system becomes inherently unstable at the operating point.[4] This fact can be verified by the eigenvalues of A_0.

Roughly speaking, the control law used in the Earth acquisition control is PD feedback,[5] i.e.,

$$\Delta u = -(K_R \Delta w + K_P e) = -K \begin{bmatrix} \Delta w \\ e \end{bmatrix} \quad (12a)$$

where

$$K = [K_R \quad K_P] \quad (12b)$$

$$K_R = \text{diag}\{(K_{Rx}, K_{Ry}, K_{Rz})\} = \begin{bmatrix} 733.5 & 0 & 0 \\ 0 & 1682.1 & 0 \\ 0 & 0 & 1667.2 \end{bmatrix} \quad (12c)$$

$$K_P = \text{diag}\{(K_{Px}, K_{Py}, K_{Pz})\} = \begin{bmatrix} 8.9 & 0 & 0 \\ 0 & 19.9 & 0 \\ 0 & 0 & 5.557 \end{bmatrix} \quad (12d)$$

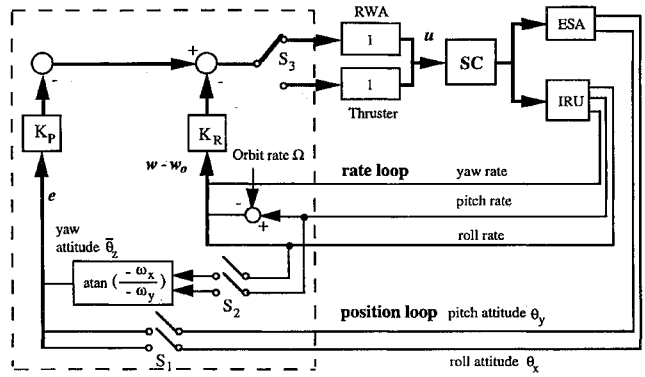

Fig. 2 EOS AM-1 Earth acquisition control system configuration.

The feedback controller gain matrix K was designed in the trade-off between system performance and stability margins. Figure 2 describes the EOS AM-1 Earth acquisition control system configuration. It has an inner-loop outer-loop structure; the ESAs are used for the position loop feedback control and the IRU is used for the rate loop. As discussed earlier, while the ESA provides the SC attitude information relative to the LVLH frame, the IRU senses the SC inertial rates (relative to the inertial frame). Hence, the IRU output signal w is subtracted by the nominal spin rate w_0 before being fed back. Since the SC yaw angle cannot be measured by any sensors, a gyrocompassing technique is used to estimate the yaw angle. After the local vertical acquisition is achieved, the SC rotation vector will be contained in the SC x–y plane; therefore, the yaw angle can be easily derived from the roll and pitch rates sensed by the IRU.

With the designed controller, the stability and stability margins of the closed-loop system can be verified by the eigenvalues of the matrix $A_c = A_0 - B_0 K$ and by the corresponding open-loop Bode plots, respectively. However, since this linear analysis is, in general, valid when the system is near the nominal operating point, further investigations are needed for the cases where the system has large attitude errors.

IV. Equilibrium Points of the Closed-Loop System

In this section, all equilibrium points of the closed-loop system will be identified for each submode. Two assumptions are made to simplify the analysis: 1) Immediately after LV/SC separation, the SC is facing down to the Earth, i.e., the angle between the SC z axis and nadir vector is not large (less than 35 deg). 2) The SC has a principal axis inertia matrix. From a practical point of view, these assumptions are reasonable. Assumption 1 ensures that the ESAs can see the Earth, whereas assumption 2 is based on the dominance of diagonal elements of the inertia matrix and the fact that the Earth acquisition control is a coarse attitude control process.

Under the first assumption the SC roll angle θ_x and pitch angle θ_y are small with respect to the LVLH frame. Therefore, the kinematics in Eqs. (3–5) can be simplified as

$$A_{zxy}(e) \cong \begin{bmatrix} \cos\theta_z & \sin\theta_z & -\theta_y \\ -\sin\theta_z & \cos\theta_z & \theta_x \\ \theta_y\cos\theta_z + \theta_x\sin\theta_z & \theta_y\sin\theta_z - \theta_x\cos\theta_z & 1 \end{bmatrix} \quad (13)$$

$$\dot{e} \cong v = w - \begin{bmatrix} \Omega\sin\theta_z \\ \Omega\cos\theta_z \\ \Omega(\theta_y\sin\theta_z - \theta_x\cos\theta_z) \end{bmatrix}$$

$$= \begin{bmatrix} \omega_x - \Omega\sin\theta_z \\ \omega_y - \Omega\cos\theta_z \\ \omega_z - \Omega(\theta_y\sin\theta_z - \theta_x\cos\theta_z) \end{bmatrix} := f_2(w, e) \quad (14)$$

Under the second assumption, the SC dynamic equation (2b) can be simplified as

$$\dot{\boldsymbol{w}} = \begin{bmatrix} \dfrac{I_{yy} - I_{zz}}{I_{xx}}\omega_y\omega_z \\ \dfrac{I_{zz} - I_{xx}}{I_{yy}}\omega_x\omega_z \\ \dfrac{I_{xx} - I_{yy}}{I_{zz}}\omega_x\omega_y \end{bmatrix} + I^{-1}\boldsymbol{u} := \boldsymbol{f}_1(\boldsymbol{w}, \boldsymbol{e}) \tag{15}$$

where

$$\boldsymbol{u} = \boldsymbol{u}_0 + \Delta\boldsymbol{u} = \Delta\boldsymbol{u} = K\begin{bmatrix} \boldsymbol{w} - \boldsymbol{w}_0 \\ \boldsymbol{e} \end{bmatrix}$$

Note that Eqs. (14) and (15) constitute the fundamental mathematical models of the SC stability analysis.

Equilibrium Points of Rate Nulling Submode

In the rate nulling submode, the attitude control thrusters are selected as the control actuators and only the rate errors are used for control. By switching S_3 to the lower position and leaving $S_{1,2}$ open, Fig. 2 shows the rate nulling submode configuration. Hence, the control law is

$$\boldsymbol{u} = -K_R(\boldsymbol{w} - \boldsymbol{w}_0) \tag{16}$$

To find all equilibrium points, we set $\dot{\boldsymbol{e}} = \boldsymbol{0}$ and $\dot{\boldsymbol{w}} = \boldsymbol{0}$ in Eqs. (14) and (15), which yields

$$\omega_x = \Omega\sin\theta_z \tag{17a}$$

$$\omega_y = \Omega\cos\theta_z \tag{17b}$$

$$\omega_z = \Omega(\theta_y\sin\theta_z - \theta_x\cos\theta_z) \tag{17c}$$

and

$$(I_{zz} - I_{yy})\omega_y\omega_z + K_{Rx}\omega_x = 0 \tag{18a}$$

$$(I_{xx} - I_{zz})\omega_x\omega_z + K_{Ry}(\omega_y - \Omega) = 0 \tag{18b}$$

$$(I_{yy} - I_{xx})\omega_x\omega_y + K_{Rz}\omega_z = 0 \tag{18c}$$

Substituting Eq. (17) into Eq. (18) gives

$$\{-(I_{zz} - I_{yy})\Omega^2\cos^2\theta_z\}\theta_x + \{(I_{zz} - I_{yy})\Omega^2\sin\theta_z\cos\theta_z\}\theta_y + K_{Rx}\Omega\sin\theta_z = 0 \tag{19a}$$

$$\{-(I_{xx} - I_{zz})\Omega^2\sin\theta_z\cos\theta_z\}\theta_x + \{(I_{xx} - I_{zz})\Omega^2\sin^2\theta_z\}\theta_y + K_{Ry}(\Omega\cos\theta_z - \Omega) = 0 \tag{19b}$$

$$\{-K_{Rz}\Omega\cos\theta_z\}\theta_x + \{K_{Rz}\Omega\sin\theta_z\}\theta_y + (I_{yy} - I_{xx})\Omega^2\sin\theta_z\cos\theta_z = 0 \tag{19c}$$

Since the equations are linear in θ_x and θ_y, a necessary and sufficient condition for $\{\theta_x, \theta_y\}$, to be a solution to Eq. (19) is

$$\operatorname{rank}\begin{bmatrix} -(I_{zz} - I_{yy})\Omega^2\cos^2\theta_z & (I_{zz} - I_{yy})\Omega^2\sin\theta_z\cos\theta_z \\ -(I_{xx} - I_{zz})\Omega^2\sin\theta_z\cos\theta_z & (I_{xx} - I_{zz})\Omega^2\sin^2\theta_z \\ -K_{Rz}\Omega\cos\theta_z & K_{Rz}\Omega\sin\theta_z \end{bmatrix}$$

$$= \operatorname{rank}\begin{bmatrix} -(I_{zz} - I_{yy})\Omega^2\cos^2\theta_z & (I_{zz} - I_{yy})\Omega^2\sin\theta_z\cos\theta_z & K_{Rx}\Omega\sin\theta_z \\ -(I_{xx} - I_{zz})\Omega^2\sin\theta_z\cos\theta_z & (I_{xx} - I_{zz})\Omega^2\sin^2\theta_z & K_{Ry}(\Omega\cos\theta_z - \Omega) \\ -K_{Rz}\Omega\cos\theta_z & K_{Rz}\Omega\sin\theta_z & (I_{yy} - I_{xx})\Omega^2\sin\theta_z\cos\theta_z \end{bmatrix} \tag{20}$$

It is easy to check that the left-hand side of Eq. (20) equals 1. Hence, for this equation to be satisfied, it is necessary (but not sufficient) for Δ_{21} to be zero, i.e.,

$$\Delta_{21} = \begin{vmatrix} (I_{zz} - I_{yy})\Omega^2\sin\theta_z\cos\theta_z & K_{Rx}\Omega\sin\theta_z \\ K_{Rz}\Omega\sin\theta_z & (I_{yy} - I_{xx})\Omega^2\sin\theta_z\cos\theta_z \end{vmatrix}$$

$$= \Omega^2\sin^2\theta_z\{(I_{zz} - I_{yy})(I_{yy} - I_{xx})\Omega^2\cos^2\theta_z - K_{Rx}K_{Rz}\} = 0 \tag{21}$$

where Δ_{21} is the (2, 1)th cofactor of the matrix in the right-hand side of Eq. (20). Using the EOS AM-1 mass properties and the controller gains, Eq. (21) only has two solutions: $\theta_z = 0$ and 180 deg. By further checking the rank of the right-hand side of Eq. (20) with $\theta_z = 0$ and 180, it can be shown that $\theta_z = 0$ is the only solution. Using $\theta_z = 0$ in Eqs. (19) and (17), the equilibrium point can be obtained as

$$\boldsymbol{e}_e = \begin{bmatrix} \theta_x \\ \theta_y \\ \theta_z \end{bmatrix} = \begin{bmatrix} 0 \\ \Phi \\ 0 \end{bmatrix}, \qquad \boldsymbol{w}_e = \begin{bmatrix} \omega_x \\ \omega_y \\ \omega_z \end{bmatrix} = \begin{bmatrix} 0 \\ \Omega \\ 0 \end{bmatrix} \tag{22}$$

where Φ is an arbitrary small number. Note that Eq. (22) is, in fact, an equilibrium line (i.e., nonisolated equilibrium points) centered at the system nominal operating point where $\Phi = 0$. In other words, every point on the line is an equilibrium point. The physical meaning is obvious: in the gyro-thruster-controlled rate nulling submode the SC may have nonzero steady-state pitch attitude error, because the gyro will not provide any error information as long as the SC is rotating about its y axis at the nominal orbit rate without having any roll and yaw attitude errors.

Equilibrium Points of Local Vertical Acquisition Submode

By closing S_1 and switching S_3 to the upper position, Fig. 2 is in the local vertical acquisition control submode configuration, i.e.,

$$\boldsymbol{u} = -\left(K_P\begin{bmatrix} \theta_x \\ \theta_y \\ 0 \end{bmatrix} + K_R(\boldsymbol{w} - \boldsymbol{w}_0)\right) = -[K_{\mathrm{PLV}}\boldsymbol{e} + K_R(\boldsymbol{w} - \boldsymbol{w}_0)] \tag{23}$$

where $K_{\mathrm{PLV}} := \operatorname{diag}\{(K_{Px}, K_{Py}, 0)\}$. By setting $\dot{\boldsymbol{e}} = \boldsymbol{0}$ and $\dot{\boldsymbol{w}} = \boldsymbol{0}$ in Eqs. (14) and (15), we have

$$\{K_{Px} - (I_{zz} - I_{yy})\Omega^2\cos^2\theta_z\}\theta_x + \{(I_{zz} - I_{yy})\Omega^2\sin\theta_z\cos\theta_z\}\theta_y + K_{Rx}\Omega\sin\theta_z = 0 \tag{24a}$$

$$\{-(I_{xx} - I_{zz})\Omega^2\sin\theta_z\cos\theta_z\}\theta_x + \{K_{Py} + (I_{xx} - I_{zz})\Omega^2\sin^2\theta_z\}\theta_y + K_{Ry}(\Omega\cos\theta_z - \Omega) = 0 \tag{24b}$$

$$\{-K_{Rz}\Omega\cos\theta_z\}\theta_x + \{K_{Rz}\Omega\sin\theta_z\}\theta_y + (I_{yy} - I_{xx})\Omega^2\sin\theta_z\cos\theta_z = 0 \tag{24c}$$

Again, Eq. (24) are linear algebraic equations for $\{\theta_x, \theta_y\}$, which have solutions if and only if

$$\text{rank}\begin{bmatrix} K_{Px} - (I_{zz} - I_{yy})\Omega^2 \cos^2\theta_z & (I_{zz} - I_{yy})\Omega^2 \sin\theta_z \cos\theta_z \\ -(I_{xx} - I_{zz})\Omega^2 \sin\theta_z \cos\theta_z & K_{Py} + (I_{xx} - I_{zz})\Omega^2 \sin^2\theta_z \\ -K_{Rz}\Omega \cos\theta_z & K_{Rz}\Omega \sin\theta_z \end{bmatrix}$$

$$= \text{rank}\begin{bmatrix} K_{Px} - (I_{zz} - I_{yy})\Omega^2 \cos^2\theta_z & (I_{zz} - I_{yy})\Omega^2 \sin\theta_z \cos\theta_z & K_{Rx}\Omega \sin\theta_z \\ -(I_{xx} - I_{zz})\Omega^2 \sin\theta_z \cos\theta_z & K_{Py} + (I_{xx} - I_{zz})\Omega^2 \sin^2\theta_z & K_{Ry}(\Omega \cos\theta_z - \Omega) \\ -K_{Rz}\Omega \cos\theta_z & K_{Rz}\Omega \sin\theta_z & (I_{yy} - I_{xx})\Omega^2 \sin\theta_z \cos\theta_z \end{bmatrix} \tag{25}$$

For this equation to be satisfied, we must have

$$\begin{vmatrix} K_{Px} - (I_{zz} - I_{yy})\Omega^2 \cos^2\theta_z & (I_{zz} - I_{yy})\Omega^2 \sin\theta_z \cos\theta_z & K_{Rx}\Omega \sin\theta_z \\ -(I_{xx} - I_{zz})\Omega^2 \sin\theta_z \cos\theta_z & K_{Py} + (I_{xx} - I_{zz})\Omega^2 \sin^2\theta_z & K_{Ry}(\Omega \cos\theta_z - \Omega) \\ -K_{Rz}\Omega \cos\theta_z & K_{Rz}\Omega \sin\theta_z & (I_{yy} - I_{xx})\Omega^2 \sin\theta_z \cos\theta_z \end{vmatrix} = \sin\theta_z\left(a_1 \cos^3\theta_z + a_2 \cos\theta_z + a_3\right) = 0 \tag{26}$$

where

$$a_1 = \Omega^4[K_{Px}(I_{xx} - I_{zz})(I_{xx} - I_{yy}) + K_{Py}(I_{zz} - I_{yy})(I_{xx} - I_{yy})] \tag{27a}$$

$$a_2 = \Omega^2\big[K_{Px}K_{Py}(I_{yy} - I_{xx}) + K_{Px}(I_{xx} - I_{zz})(I_{yy} - I_{xx})\Omega^2 - K_{Px}K_{Ry}K_{Rz} + K_{Rx}K_{Py}K_{Rz}\big] \tag{27b}$$

$$a_3 = \Omega^2 K_{Px}K_{Ry}K_{Rz} \tag{27c}$$

For the fixed EOS AM-1 mass properties and controller, Eq. (26) only has two solutions: $\theta_z = 0$ and 180 deg. Using these two values in Eqs. (24) and (17), two equilibrium points can be found for the local vertical control system.

Equilibrium point 1:

$$\boldsymbol{e}_{e1} = \begin{bmatrix} 0 \\ 0 \\ 0 \end{bmatrix}, \qquad \boldsymbol{w}_{e1} = \begin{bmatrix} 0 \\ \Omega \\ 0 \end{bmatrix} \tag{28a}$$

Equilibrium point 2:

$$\boldsymbol{e}_{e2} = \begin{bmatrix} 0 \\ \dfrac{2K_{Ry}\Omega}{K_{Py}} \\ 180 \end{bmatrix}, \qquad \boldsymbol{w}_{e2} = \begin{bmatrix} 0 \\ -\Omega \\ 0 \end{bmatrix} \tag{28b}$$

Note that equilibrium point 1 is the nominal operating point. At the second equilibrium point, the SC has 180-deg yaw error and −9.7-deg pitch error. The nonzero steady-state pitch attitude error is created to compensate for the opposite pitch rate bias $\boldsymbol{w}_0$, because the SC is flying backwards. This steady-state error can be verified by the single axis analysis and the fact that in the steady-state the control torque is zero, i.e.,

$$u_y = -K_{Py}\theta_{e2y} - K_{Ry}(\omega_{e2y} - \Omega) = 0$$

Equilibrium Points of Yaw Acquisition Submode

By further closing S_2, Fig. 2 is in the yaw acquisition control submode configuration, i.e.,

$$\boldsymbol{u} = -\left(K_P \begin{bmatrix} \theta_x \\ \theta_y \\ \bar{\theta}_z \end{bmatrix} + K_R(\boldsymbol{w} - \boldsymbol{w}_0)\right) \tag{29}$$

whereas θ_x and θ_y are obtained directly from the ESAs, the estimated SC yaw attitude $\bar{\theta}_z$ is derived from the gyro information (gyrocompassing)

$$\bar{\theta}_z = \arctan\left(\frac{\omega_x/\Omega}{\omega_y/\Omega}\right), \qquad -180 < \bar{\theta}_z \le 180$$

By setting $\dot{\boldsymbol{e}} = \boldsymbol{0}$ and $\dot{\boldsymbol{w}} = \boldsymbol{0}$ in Eqs. (14) and (15), we have

$$(I_{zz} - I_{yy})\omega_y\omega_z + K_{Px}\theta_x + K_{Rx}\omega_x = 0 \tag{30a}$$

$$(I_{xx} - I_{zz})\omega_x\omega_z + K_{Py}\theta_y + K_{Ry}(\omega_y - \Omega) = 0 \tag{30b}$$

$$(I_{yy} - I_{xx})\omega_x\omega_y + K_{Pz}\arctan\left(\frac{\omega_x/\Omega}{\omega_y/\Omega}\right) + K_{Rz}\omega_z = 0 \tag{30c}$$

Note that in the steady state, $\arctan[(\omega_x/\Omega), (\omega_y/\Omega)] = \theta_z$ [refer to Eq. (17)]. Hence, Eq. (30) can be further simplified as

$$\left\{K_{Px} - (I_{zz} - I_{yy})\Omega^2 \cos^2\theta_z\right\}\theta_x + \left\{(I_{zz} - I_{yy})\Omega^2 \sin\theta_z \cos\theta_z\right\}\theta_y + K_{Rx}\Omega \sin\theta_z = 0 \tag{31a}$$

$$\left\{-(I_{xx} - I_{zz})\Omega^2 \sin\theta_z \cos\theta_z\right\}\theta_x + \left\{K_{Py} + (I_{xx} - I_{zz})\Omega^2 \sin^2\theta_z\right\}\theta_y + K_{Ry}(\Omega \cos\theta_z - \Omega) = 0 \tag{31b}$$

$$\left\{-K_{Rz}\Omega \cos\theta_z\right\}\theta_x + \left\{K_{Rz}\Omega \sin\theta_z\right\}\theta_y + K_{Pz}\theta_z + (I_{yy} - I_{xx})\Omega^2 \sin\theta_z \cos\theta_z = 0 \tag{31c}$$

The rank condition for Eq. (31) to have solutions for θ_x and θ_y is

$$\text{rank}\begin{bmatrix} K_{Px} - (I_{zz} - I_{yy})\Omega^2 \cos^2\theta_z & (I_{zz} - I_{yy})\Omega^2 \sin\theta_z \cos\theta_z \\ -(I_{xx} - I_{zz})\Omega^2 \sin\theta_z \cos\theta_z & K_{Py} + (I_{xx} - I_{zz})\Omega^2 \sin^2\theta_z \\ -K_{Rz}\Omega \cos\theta_z & K_{Rz}\Omega \sin\theta_z \end{bmatrix}$$

$$= \text{rank}\begin{bmatrix} K_{Px} - (I_{zz} - I_{yy})\Omega^2 \cos^2\theta_z & (I_{zz} - I_{yy})\Omega^2 \sin\theta_z \cos\theta_z & K_{Rx}\Omega \sin\theta_z \\ -(I_{xx} - I_{zz})\Omega^2 \sin\theta_z \cos\theta_z & K_{Py} + (I_{xx} - I_{zz})\Omega^2 \sin^2\theta_z & K_{Ry}(\Omega \cos\theta_z - \Omega) \\ -K_{Rz}\Omega \cos\theta_z & K_{Rz}\Omega \sin\theta_z & K_{Pz}\theta_z + (I_{yy} - I_{xx})\Omega^2 \sin\theta_z \cos\theta_z \end{bmatrix} \tag{32}$$

To satisfy this equation, we must have

$$\begin{bmatrix} K_{Px} - (I_{zz} - I_{yy})\Omega^2 \cos^2\theta_z & (I_{zz} - I_{yy})\Omega^2 \sin\theta_z \cos\theta_z & K_{Rx}\Omega \sin\theta_z \\ -(I_{xx} - I_{zz})\Omega^2 \sin\theta_z \cos\theta_z & K_{Py} + (I_{xx} - I_{zz})\Omega^2 \sin^2\theta_z & K_{Ry}(\Omega\cos\theta_z - \Omega) \\ -K_{Rz}\Omega\cos\theta_z & K_{Rz}\Omega\sin\theta_z & K_{Pz}\theta_z + (I_{yy} - I_{xx})\Omega^2 \sin\theta_z \cos\theta_z \end{bmatrix}$$

$$= \sin\theta_z\left(a_1 \cos^3\theta_z + a_2 \cos\theta_z + a_3\right) + \theta_z\left(b_1 + b_2 \sin^2\theta_z\right) = 0 \tag{33}$$

where a_1, a_2, and a_3 are given in Eq. (27), and

$$b_1 = \left[K_{Px}K_{Py}K_{Pz} - K_{Py}K_{Pz}(I_{zz} - I_{yy})\Omega^2\right]$$

$$b_2 = \left[K_{Px}K_{Pz}(I_{xx} - I_{zz}) + K_{Py}K_{Pz}(I_{zz} - I_{yy})\right]\Omega^2$$

By using the deployed mass properties (see Table 1), one can find that only one solution exists to Eq. (33), which is $\theta_z = 0$. Then from Eqs. (31) and (17), the equilibrium point of the yaw acquisition control system is obtained as

$$\boldsymbol{e}_e = \begin{bmatrix} 0 \\ 0 \\ 0 \end{bmatrix}, \qquad \boldsymbol{w}_e = \begin{bmatrix} 0 \\ \Omega \\ 0 \end{bmatrix} \tag{34}$$

which is the system nominal operating point.

V. Stability of the Closed-Loop System

The basic approach in this section is to linearize the closed-loop system at each equilibrium point, then check the eigenvalues of the resulting A matrix. To this end, we rewrite Eqs. (15) and (14) as

$$\dot{\boldsymbol{w}} = -I^{-1}[\boldsymbol{w}]_s I\boldsymbol{w} - I^{-1}K_R(\boldsymbol{w} - \boldsymbol{w}_0) - I^{-1}K_P\boldsymbol{e} := \boldsymbol{f}_1(\boldsymbol{w}, \boldsymbol{e}) \tag{35}$$

$$\dot{\boldsymbol{e}} = \boldsymbol{w} - \begin{bmatrix} \Omega\sin\theta_z \\ \Omega\cos\theta_z \\ \Omega(\theta_y \sin\theta_z - \theta_x\cos\theta_z) \end{bmatrix} := \boldsymbol{f}_2(\boldsymbol{w}, \boldsymbol{e}) \tag{36}$$

Taking the derivative of Eqs. (35) and (36) with respect to $\boldsymbol{w}$ and $\boldsymbol{e}$, we have the following linearized Jacobian equation at equilibrium point $(\boldsymbol{w}_e, \boldsymbol{e}_e)$:

$$\begin{bmatrix} \Delta\dot{\boldsymbol{w}} \\ \Delta\dot{\boldsymbol{e}} \end{bmatrix} = \begin{bmatrix} \dfrac{\partial \boldsymbol{f}_1}{\partial \boldsymbol{w}}(\boldsymbol{w}_e, \boldsymbol{e}_e) & \dfrac{\partial \boldsymbol{f}_1}{\partial \boldsymbol{e}}(\boldsymbol{w}_e, \boldsymbol{e}_e) \\ \dfrac{\partial \boldsymbol{f}_2}{\partial \boldsymbol{w}}(\boldsymbol{w}_e, \boldsymbol{e}_e) & \dfrac{\partial \boldsymbol{f}_2}{\partial \boldsymbol{e}}(\boldsymbol{w}_e, \boldsymbol{e}_e) \end{bmatrix} \begin{bmatrix} \Delta\boldsymbol{w} \\ \Delta\boldsymbol{e} \end{bmatrix} := A_c \begin{bmatrix} \Delta\boldsymbol{w} \\ \Delta\boldsymbol{e} \end{bmatrix} \tag{37}$$

where

$$\Delta\boldsymbol{w} = \boldsymbol{w} - \boldsymbol{w}_e \qquad \Delta\boldsymbol{e} = \boldsymbol{e} - \boldsymbol{e}_e$$

$$\frac{\partial \boldsymbol{f}_1}{\partial \boldsymbol{w}}(\boldsymbol{w}, \boldsymbol{e}) = I^{-1}([I\boldsymbol{w}]_s - [\boldsymbol{w}]_s I) - I^{-1}K_R$$

$$\frac{\partial \boldsymbol{f}_1}{\partial \boldsymbol{e}}(\boldsymbol{w}, \boldsymbol{e}) = -I^{-1}K_P \qquad \frac{\partial \boldsymbol{f}_2}{\partial \boldsymbol{w}}(\boldsymbol{w}, \boldsymbol{e}) = 1_3$$

$$\frac{\partial \boldsymbol{f}_2}{\partial \boldsymbol{e}}(\boldsymbol{w}, \boldsymbol{e}) = \begin{bmatrix} 0 & 0 & -\Omega\cos\theta_z \\ 0 & 0 & -\Omega\sin\theta_z \\ \Omega\cos\theta_z & -\Omega\sin\theta_z & -\Omega(\theta_y\cos\theta_z + \theta_x\sin\theta_z) \end{bmatrix}$$

Note that $\dot{\boldsymbol{w}}_e = \boldsymbol{f}_1(\boldsymbol{w}_e, \boldsymbol{e}_e) = \boldsymbol{0}$ and $\dot{\boldsymbol{e}}_e = \boldsymbol{f}_2(\boldsymbol{w}_e, \boldsymbol{e}_e) = \boldsymbol{0}$, since $(\boldsymbol{w}_e, \boldsymbol{e}_e)$ is an equilibrium point.

Stability of Rate Nulling Submode

As mentioned in the preceding section, Eq. (22) is in fact an equilibrium line centered at the system nominal operating point where $\Phi = 0$. Evaluating the A matrix in Eq. (37) at any point on the line, we have

$$A_c = \begin{bmatrix} A_{c11} & 0_3 \\ 1_3 & A_{c22} \end{bmatrix} \tag{38a}$$

where

$$A_{c11} = I^{-1}([I\boldsymbol{w}_0]_s - [\boldsymbol{w}_0]_s I) - I^{-1}K_R \tag{38b}$$

$$A_{c22} = \begin{bmatrix} 0 & 0 & -\Omega \\ 0 & 0 & 0 \\ \Omega & 0 & -\Omega\Phi \end{bmatrix} \tag{38c}$$

Therefore, the state-space representation of the linearized system at any point on the equilibrium line of Eq. (22) is

$$\dot{\boldsymbol{x}}(t) = A_c\boldsymbol{x}(t) \tag{39}$$

with its homogeneous solution

$$\boldsymbol{x}(t) = e^{-A_c t}\boldsymbol{x}(0) \tag{40}$$

where

$$\boldsymbol{x} = \begin{bmatrix} \Delta\boldsymbol{w} \\ \Delta\boldsymbol{e} \end{bmatrix}$$

The eigenvalues of the system at an equilibrium point consist of

$$\text{eigen}(A_{c11}) = \{-1.005e-01, -1.214e-01, -8.198e-02\} \tag{41a}$$

and

$$\text{eigen}(A_{c22}) = \left\{0, \frac{-\Omega\Phi \pm \Omega\sqrt{4 - \Phi^2 i}}{2}\right\} \tag{41b}$$

Apparently, the stability of the linearized system depends on the value of Φ. If $\Phi > 0$, A_{c22} has a pair of unstable eigenvalues; therefore, the corresponding equilibrium point is an unstable one. If $\Phi < 0$, there are no unstable eigenvalues. As Φ goes to zero, the pair of the conjugate eigenvalues of A_{c22} moves to the imaginary axis. By further investigating the eigenstructure of A_{c22}, one can see that the eigenspace of the zero eigenvalue of A_{c22} [Eq. (41b)] is

$$S_1 = \text{span}\left\{\begin{bmatrix} 0 \\ 1 \\ 0 \end{bmatrix}\right\} \tag{42a}$$

The eigenspace of the conjugate eigenvalues in Eq. (41b) is

$$S_{2,3} = \text{span}\left\{\begin{bmatrix} 1 \\ 0 \\ 0 \end{bmatrix}, \begin{bmatrix} 0 \\ 0 \\ 1 \end{bmatrix}\right\} \tag{42b}$$

This means that if $\Phi > 0$, then the $S_{2,3}$ is the system's unstable subspace[6]: if the initial SC attitude has any roll and/or yaw errors with a positive pitch error, the system will diverge in the combined roll and yaw direction [refer to Eq. (40)]. If the initial SC attitude has a negative pitch error, a small initial roll and/or yaw error would converge to zero. However, since the pitch error is an uncontrollable state corresponding to the zero eigenvalue, in the real situation, because of the high-order terms of Eq. (36) and external disturbances, the pitch attitude will drift out of the linear region and the 3-axis attitude will in general diverge. On the other hand, the 3-axis SC body rates are controllable states; their eigenvalues can be arbitrarily assigned by the K_R [refer to A_{c11} in Eq. (38b)]. Therefore, any initial rate errors can be reduced to zero by the control system.

The plots in Fig. 3 are the simulation results of the gyro-thruster-controlled rate nulling control system. These plots are generated from a high-fidelity spacecraft simulator EOSSIM, which has been

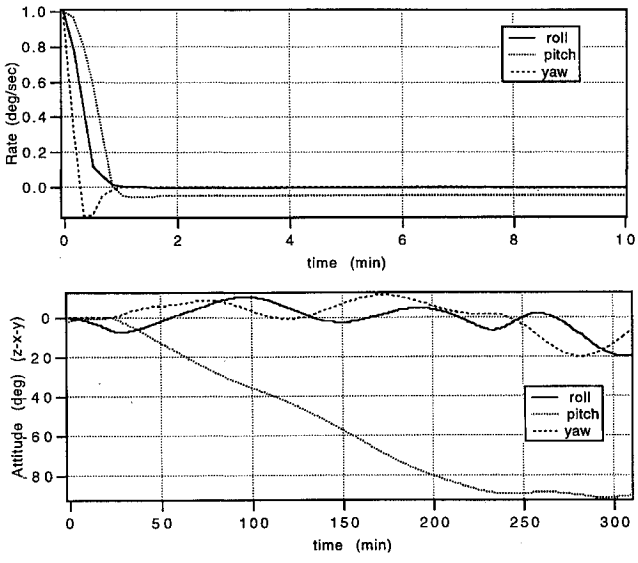

Fig. 3 Rate nulling submode performance

used for the EOS AM-1 control system design. The simulation results demonstrate that although SC rate errors can be controlled to zero, the attitude motion is unstable. Therefore, according to the analysis, the SC should be switched to the local vertical acquisition submode as soon as possible after the SC body rate is reduced.

Stability of Local Vertical Submode

Evaluating Eq. (37) at Eq. (28a), which is the system nominal operating point, we have

$$A_c = \begin{bmatrix} I^{-1}([Iw_0]_s - [w_0]_s I) - I^{-1}K_R & -I^{-1}K_{\text{PLV}} \\ 1_3 & -[w_0]_s \end{bmatrix} \tag{43}$$

The eigenvalues of A_c are $\{-1.068e-01, -1.331e-02, -1.435e-02, -7.599e-02, -9.486e-02, -8.649e-05\}$, which implies that the system nominal operating point is an asymptotically stable equilibrium point in the local vertical acquisition submode.

The same procedure can be applied to linearize the system at the second equilibrium point, where the SC has a 180-deg yaw error. Evaluating Eq. (37) at Eq. (28b), we have

$$A_c = \begin{bmatrix} I^{-1}([Iw_{e2}]_s - [w_{e2}]_s I) - I^{-1}K_R & -I^{-1}K_{\text{PLV}} \\ 1_3 & A_{c22} \end{bmatrix} \tag{44a}$$

where

$$A_{c22} = \begin{bmatrix} 0 & 0 & \Omega \\ 0 & 0 & 0 \\ -\Omega & 0 & 2\Omega\dfrac{K_{Ry}}{K_{Py}} \end{bmatrix} \tag{44b}$$

The eigenvalues of A_c are $\{-1.068e-01, -1.331e-02, -1.435e-02, -7.599e-02, -9.486e-02, 8.362e-05\}$. Since a positive eigenvalue exists, the second equilibrium point is an unstable equilibrium point.

This analysis indicates that there is only one stable equilibrium point in the local vertical acquisition submode, and the system will converge to the nominal operation point from any yaw angle. However, the convergence rate is very slow, as shown in Fig. 4, because of the existence of an eigenvalue that is very close to the imaginary axis for both equilibrium points.

Stability of Yaw Acquisition Submode

Evaluating Eq. (37) at Eq. (34), which is the system nominal attitude, we have

$$A_c = \begin{bmatrix} I^{-1}([Iw_0]_s - [w_0]_s I) - I^{-1}K_R & -I^{-1}K_P \\ 1_3 & -[w_0]_s \end{bmatrix} \tag{45}$$

Table 2 Time line highlights of Fig. 6

min. 0:	Perigee. LV/SC separation. Rate nulling submode commanded by the SCC 3 s after the separation. Thruster control.
min. 0.5:	Rate nulling complete. Local vertical acquisition submode begins. RWA control.
min. 1:	Solar array hinge deployment begins.
min. 3:	Solar array hinge deployment complete. Momentum transfer between the hinge and SC main body causes attitude disturbance.
min. 4:	Local vertical acquisition submode complete. Yaw acquisition submode commanded by the SCC. RWA control. Solar array blanket deployment begins.
min. 8:	Yaw acquisition submode complete.

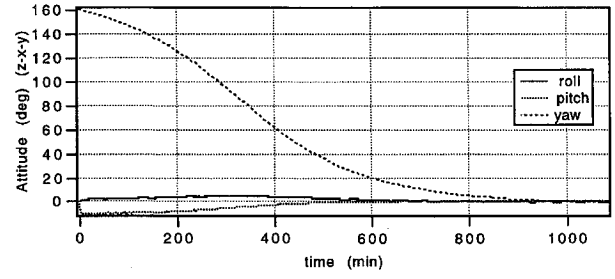

Fig. 4 Local vertical acquisition submode, attitude errors.

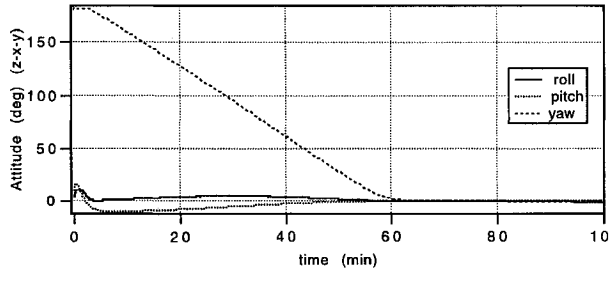

Fig. 5 Yaw acquisition submode, attitude errors.

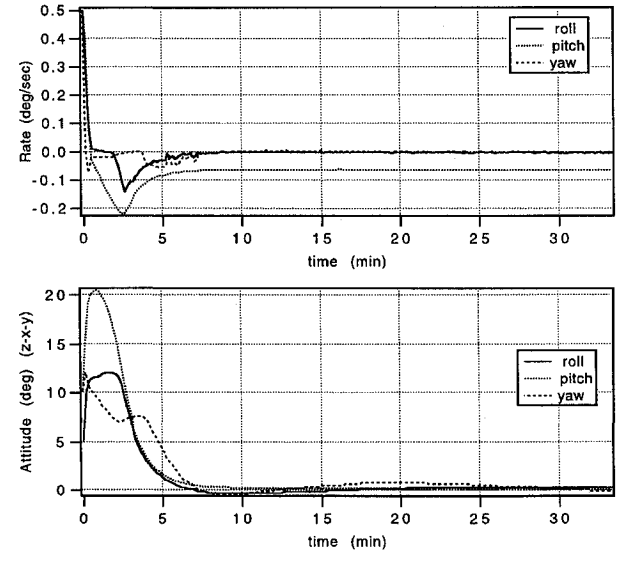

Fig. 6 Earth acquisition mode performance.

The eigenvalues of A_c are $\{-1.081e-01, -6.718e-02, -1.469e-02, -9.707e-02, -1.328e-02, -3.568e-03\}$, which implies that the yaw acquisition control system is asymptotically stable with large yaw attitude errors. Since the yaw attitude error is used for feedback in this submode, the system bandwidth has greatly increased. This fact can be seen from Fig. 5.

Stability of Earth Acquisition Mode

In this subsection, simulation results are presented for a typical EOS AM-1 initial acquisition control case. More information on

different simulation scenarios can be found in Ref. 2. In the following simulation, the initial SC attitude errors and body rates are: roll error = 5.0 deg, pitch error = 10.0 deg, yaw error = 10.0 deg, roll rate = 0.5 deg/s, pitch rate = 0.5 deg/s, and yaw rate = 0.5 deg/s. Referring to Fig. 6, the time line highlights are listed in Table 2.

VI. Conclusions

The design and analysis of the EOS AM-1 spacecraft Earth acquisition attitude control have been provided. The system nonlinear dynamic and kinematic equations were simplified under two assumptions: immediately after LV/SC separation the SC is facing down to the Earth and the SC has a principal axis inertia matrix. Based on the simplified nonlinear model, all system equilibrium points were identified for all three control configurations. Then the stability associated with each of the equilibrium points was investigated. In the rate nulling submode, an equilibrium line centered at the system nominal operating point exists. Although the system is not asymptotically stable in this submode, the SC 3-axis rate vector is in the system's stable subspace. The analysis suggested that the system be switched to the local vertical acquisition mode as soon as possible after the SC body rate is reduced. In the local vertical submode, two equilibrium points exist: one is the system nominal operating point, which is stable, and the other is 180 deg in yaw from the nominal orientation, which is unstable. As shown by the analysis and confirmed by high-fidelity simulation, the SC can always converge to the nominal operating point from any yaw angles. However, the convergence rate is slow in this submode since no yaw attitude errors are used for feedback control. In the yaw acquisition submode, only one equilibrium point exists, which is the system nominal operating point and is asymptotically stable. Since the yaw attitude error is added to the control system, the system bandwidth is much higher than the local vertical acquisition control system.

This paper has extended the results from the previously performed linear system stability analysis and provided a deeper understanding to the system dynamics. The results are useful for analyzing off-nominal LV/SC separation and in determining the submode transition thresholds.

Acknowledgments

This work was completed during the course of the EOS AM-1 spacecraft attitude control and attitude determination design and flight software implementation under NASA Contract EOS AM NAS5-32500. The authors are grateful to M. Hughes, G. Shareshian, J. Tralie, and M. Laraia of Lockheed Martin Astro Space, P. Kudva of McDonnell Douglas Aerospace, and S. Lee of Honeywell for their inspiring discussions and valuable support.

References

[1]Boka, J. B., "Earth Observing Satellite (EOS) Initial Earth Acquisition," General Electric Co. Astro Space, EOS-DN-GNC-035, Princeton, NJ, Sept. 1992.

[2]Li, X., "EOS-AM Earth Acquisition Design," Martin Marietta Astro Space, EOS-DN-GNC-067, Princeton, NJ, April 1994.

[3]Wertz, J., *Spacecraft Attitude Determination and Control*, Kluwer Academic, Dordrecht, The Netherlands, 1978.

[4]Greenwood, D. T., *Principles of Dynamics*, 2nd ed., Prentice–Hall, Englewood Cliffs, NJ, 1988.

[5]Ogata, K., *Modern Control Engineering*, Prentice–Hall, Englewood Cliffs, NJ, 1970.

[6]Kwakernaak, H., and Sivan, R., *Linear Optimal Control Systems*, Wiley-Interscience, New York, 1972.